

Numerical approximation of (crystalline) anisotropic surface diffusion

Robert Nürnberg

Department of Mathematics
Imperial College London

Mathematical Aspects of Surface and Interface Dynamics
Tokyo, 25–27 October 2017

Isotropic surface diffusion in the plane

Evolving simple (embedded - no intersections) planar closed curve $\Gamma(t)$.

Let $\vec{x}(\rho, t)$, $\rho \in I := \mathbb{R}/\mathbb{Z}$ (periodic $[0, 1]$), be a parameterization of $\Gamma(t)$.

Arclength $s \rightarrow$ unit tangent $\vec{\tau} = \vec{x}_s = \frac{\vec{x}_\rho}{|\vec{x}_\rho|}$.

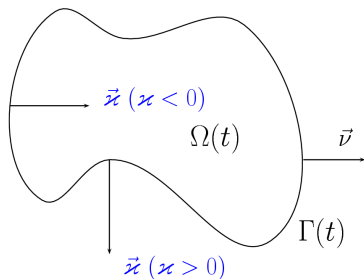
Curvature vector $\vec{\kappa} = \vec{\tau}_s = \vec{x}_{ss} = \frac{1}{|\vec{x}_\rho|} \left(\frac{\vec{x}_\rho}{|\vec{x}_\rho|} \right)_\rho$.

Unit normal $\vec{\nu} \rightarrow \vec{\kappa} \equiv \varkappa \vec{\nu}$, where \varkappa is the curvature.

Let $D(t)$ be the region bounded by $\Gamma(t)$.

If $\vec{\nu}$ is the outward normal, then \varkappa is negative if $D(t)$ is locally convex.

Isotropic surface diffusion in the plane



For the evolution of $\Gamma(t)$, it suffices to prescribe its normal velocity

$$\mathcal{V} \equiv \vec{x}_t \cdot \vec{\nu}.$$

Note that tangential velocities just change the parameterization $\vec{x}(\rho, t)$.

Surface diffusion: $\mathcal{V} = -\kappa_{SS}$

Isotropic surface diffusion in the plane

$$\mathcal{V} = -\kappa_{SS}$$

Surface diffusion has important applications in e.g. Materials Science. It is the H^{-1} gradient flow for the energy $|\Gamma(t)|$, and so it has the following properties.

$$\frac{d}{dt} |\Gamma(t)| = - \int_{\Gamma(t)} \mathcal{V} \kappa \, ds = - \int_{\Gamma(t)} (\kappa_s)^2 \, ds \equiv - \|\mathcal{V}\|_{H^{-1}(\Gamma(t))}^2 \leq 0.$$

$$\frac{d}{dt} |D(t)| = \int_{\Gamma(t)} \mathcal{V} \, ds = - \int_{\Gamma(t)} \kappa_{SS} \, ds = 0.$$

Numerical methods for surface diffusion

Depending on how the free surface $\Gamma(t)$ is represented, there exist different types of numerical approaches:

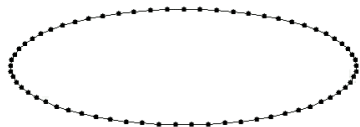
Front tracking methods: • Bower, Freund (1995); Kraft, Arzt (1997);
Xia, Bower, Suo, Shih (1997);
Dziuk, Kuwert, Schätzle (2002);
Bänsch, Morin, Nochetto (2005);
Barrett, Garcke, Nürnberg (2007); ...

Phase field methods: • Mahadevan, Bradley (1999);
Bhate, Kumar, Bower (2000);
Barrett, Nürnberg, Styles (2004);
Barrett, Garcke, Nürnberg (2006); ...

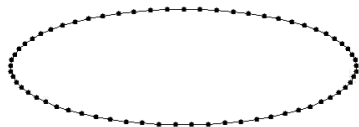
Level set methods: • Chopp, Sethian (1999); Li, Zhao, Gao (1999);
Averbuch, Israeli, Ravve, Yavneh (2001); ...

Front tracking methods

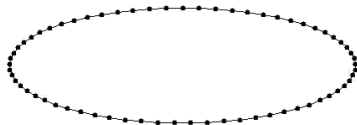
The discrete tangential motion induced by the numerical scheme can lead to coalescence in practice.



DKS



BMN



BGN

BGN formulation

Dziuk, Kuwert, Schätzle (2002) is based on the formulation

$$\vec{x}_t = -\kappa_{SS} \vec{\nu} \equiv -\vec{\kappa}_{SS} - \frac{3}{2} (|\vec{\kappa}|^2 \vec{x}_s)_s + \frac{1}{2} |\vec{\kappa}|^2 \vec{\kappa}, \quad \vec{\kappa} = \vec{x}_{SS}.$$

Bänsch, Morin, Nochetto (2005) is based on the formulation

$$\vec{x}_t = \mathcal{V} \vec{\nu}, \quad \mathcal{V} = -\kappa_{SS}, \quad \kappa = \vec{\kappa} \cdot \vec{\nu}, \quad \vec{\kappa} = \vec{x}_{SS}.$$

Both approaches have in common that they evolve the parameterization \vec{x} only in the *normal* direction.

We use the following formulation of surface diffusion:

$$\vec{x}_t \cdot \vec{\nu} = -\kappa_{SS}, \quad \kappa \vec{\nu} = \vec{x}_{SS}.$$

Note that because the tangential component $\psi = \vec{x}_t \cdot \vec{\tau}$ of the velocity \vec{x}_t is not prescribed, there exists a whole *family of solutions* \vec{x} , even though the evolution of Γ is uniquely determined.

Weak formulation:

For smooth test functions $\varphi \in V := H^1(\mathbb{R}/\mathbb{Z}; \mathbb{R})$ and $\vec{\varphi} \in \underline{V} := H^1(\mathbb{R}/\mathbb{Z}; \mathbb{R}^2)$ it holds that

$$\int_{\Gamma} \vec{x}_t \cdot \vec{\nu} \varphi \, ds = \int_{\Gamma} \varkappa_s \varphi_s \, ds, \quad \int_{\Gamma} \varkappa \vec{\nu} \cdot \vec{\varphi} \, ds + \int_{\Gamma} \vec{x}_s \cdot \vec{\varphi}_s \, ds = 0.$$

For the discretization, we approximate $\Gamma(t_m)$ by a polygonal curve Γ^m .

- $V^h \subset V$ and $\underline{V}^h \subset \underline{V}$ are piecewise linear finite element spaces.
- $\langle \cdot, \cdot \rangle_{\Gamma^m}$ is the L^2 -inner product on Γ^m .
- $\langle \cdot, \cdot \rangle_{\Gamma^m}^h$ is the mass-lumped L^2 -inner product on Γ^m .

Parametric finite element approximation

(\mathcal{P}^h) Find $(\vec{X}^{m+1}, \kappa^{m+1}) \in \underline{V}^h \times V^h$ such that

$$\left\langle \frac{\vec{X}^{m+1} - \vec{X}^m}{\tau_m}, \chi \vec{v}^m \right\rangle_{\Gamma^m}^h - \langle \kappa_s^{m+1}, \chi_s \rangle_{\Gamma^m} = 0 \quad \forall \chi \in V^h,$$
$$\langle \kappa^{m+1} \vec{v}^m, \vec{\eta} \rangle_{\Gamma^m}^h + \langle \vec{X}_s^{m+1}, \vec{\eta}_s \rangle_{\Gamma^m} = 0 \quad \forall \vec{\eta} \in \underline{V}^h;$$

- **Existence, Uniqueness**

Under mild assumptions on \vec{X}^m , $\exists!$ $(\vec{X}^{m+1}, \kappa^{m+1}) \in \underline{V}^h \times V^h$.

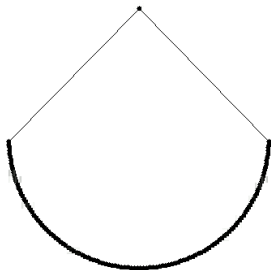
- **Stability** For all $k = 1 \rightarrow M$ it holds that

$$|\Gamma^k| + \sum_{m=0}^{k-1} \tau_m \langle \kappa_s^{m+1}, \kappa_s^{m+1} \rangle_{\Gamma^m} \leq |\Gamma^0|.$$

- **Area conservation** for a continuous in time semidiscrete scheme.
- **Equidistribution of mesh points** for $\vec{X}(t)$, where $\vec{X}(t)$ not locally parallel, for any $t > 0$, for a continuous in time semidiscrete scheme.

Equidistribution of mesh points

Although equidistribution cannot be shown for the fully discrete scheme, (eventual) equidistribution is observed in practice.



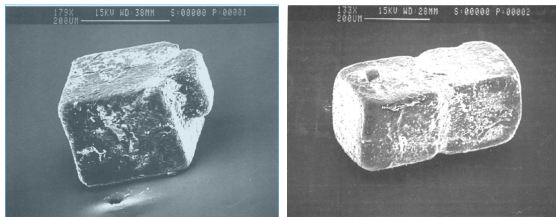
Anisotropy

For the currently chosen interface energy

$$|\Gamma| = \int_{\Gamma} 1 \, ds$$

the energy minimizers for a given area are circles.

However, in materials science and physics other shapes are of interest:



Morgan, French & Greenleaf (1988)

Salt crystals

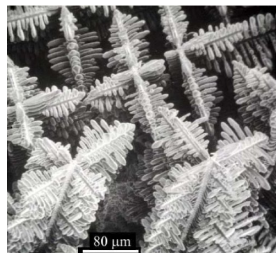
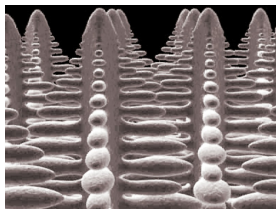
Anisotropy

For the currently chosen interface energy

$$|\Gamma| = \int_{\Gamma} 1 \, ds$$

the energy minimizers for a given area are circles.

However, in materials science and physics other shapes are of interest:



Solidification to metallic dendrites

Anisotropy

For the currently chosen interface energy

$$|\Gamma| = \int_{\Gamma} 1 \, ds$$

the energy minimizers for a given area are circles.

However, in materials science and physics other shapes are of interest:



www.snowcrystals.com

Snow crystals

Anisotropy

These crystalline shapes, and other *non-isotropic* shapes, can be modelled with an anisotropic surface energy

$$|\Gamma|_\gamma = \int_\Gamma \hat{\gamma}(\vec{\nu}) \, ds.$$

Here $\hat{\gamma} : \mathbb{S}^1 \rightarrow \mathbb{R}_{>0}$ is an *anisotropic surface energy density*, which models the effect of the underlying crystal structure on the surface energy.

For mathematical convenience, it is common to extend $\hat{\gamma}$ from \mathbb{S}^1 to all of \mathbb{R}^2 via the one-homogeneous extension

$$\gamma(\vec{z}) := |\vec{z}| \hat{\gamma}\left(\frac{\vec{z}}{|\vec{z}|}\right) \quad \forall \vec{z} \in \mathbb{R}^2 \setminus \{\vec{0}\}.$$

Assuming that $\hat{\gamma}$ is smooth and even, i.e. $\hat{\gamma}(-\vec{\nu}) = \hat{\gamma}(\vec{\nu})$, we hence obtain that $\gamma \in C^2(\mathbb{R}^2 \setminus \{\vec{0}\}) \cap C(\mathbb{R})$, with $\gamma(\vec{z}) > 0$ for $\vec{z} \neq \vec{0}$, is absolutely homogeneous of degree 1:

$$\gamma(\lambda \vec{z}) = |\lambda| \gamma(\vec{z}) \quad \forall \vec{z} \in \mathbb{R}^2, \quad \forall \lambda \in \mathbb{R}.$$

Anisotropy

Examples

- Isotropic case: $\gamma(\vec{p}) = |\vec{p}| \iff \hat{\gamma}(\vec{n}) = 1$.
- l^r -norm: $\gamma(\vec{p}) = |\vec{p}|_r = \left(\sum_{k=1}^2 |p_k|^r \right)^{\frac{1}{r}}$.
- Weighted norm: $\gamma(\vec{p}) = (\vec{p} \cdot G \vec{p})^{\frac{1}{2}}$,
for $G \in \mathbb{R}^{2 \times 2}$ symmetric, positive definite.
- Kobayashi (1993):
 $\hat{\gamma}(\vec{n}) = 1 + \delta \cos(k \theta(\vec{n}))$, $\theta(\vec{n}) = \arctan(\frac{n_2}{n_1})$, for $\delta \in \mathbb{R}_{>0}$, $k \in \mathbb{N}$.

Anisotropy

Different anisotropies can be visualized by their Frank diagram

$$\mathcal{F} := \{\vec{\rho} \in \mathbb{R}^2 : \gamma(\vec{\rho}) \leq 1\}$$

and their Wulff shape

$$\mathcal{W} := \{\vec{q} \in \mathbb{R}^2 : \gamma^*(\vec{q}) \leq 1\},$$

which was first introduced by Wulff (1901). Here γ^* is the dual to γ and is defined by

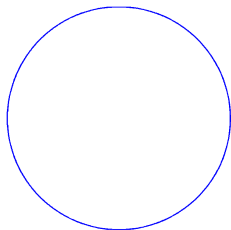
$$\gamma^*(\vec{q}) = \sup_{\vec{\rho} \in \mathbb{R}^2 \setminus \{\vec{0}\}} \frac{\vec{q} \cdot \vec{\rho}}{\gamma(\vec{\rho})} = \sup_{\vec{n} \in \mathbb{S}^1} \frac{\vec{q} \cdot \vec{n}}{\gamma(\vec{n})}.$$

Wulff shapes are always convex, and they represent the equilibrium shapes of the anisotropic surface energy. Hence they give an indication of the shape of the underlying crystal structure that is modelled.

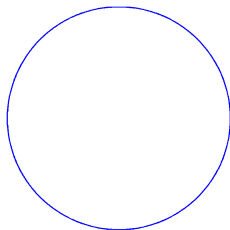
Anisotropy

Wulff shapes

- Isotropic case: $\gamma(\vec{p}) = |\vec{p}| \iff \hat{\gamma}(\vec{n}) = 1$.



Frank diagram

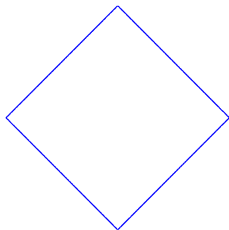


Wulff shape

Anisotropy

Wulff shapes

- l^1 -norm: $\gamma(\vec{p}) = |\vec{p}|_{l^1} = \sum_{i=1}^2 |p_i|$.



Frank diagram

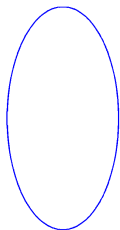


Wulff shape

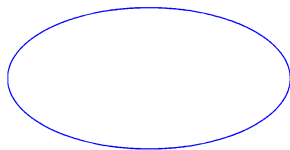
Anisotropy

Wulff shapes

- Weighted norm: $\gamma(\vec{p}) = (\vec{p} \cdot G \vec{p})^{\frac{1}{2}}$, $G = \begin{pmatrix} 1 & 0 \\ 0 & 0.25 \end{pmatrix}$.



Frank diagram



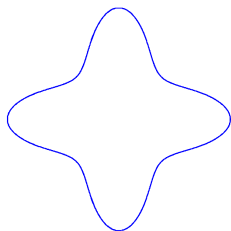
Wulff shape

Anisotropy

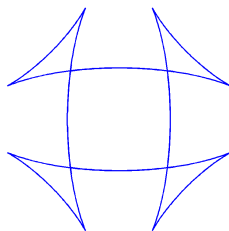
Wulff shapes

- Kobayashi (1993):

$$\hat{\gamma}(\vec{n}) = 1 - 0.3 \cos(4\theta(\vec{n})), \quad \theta(\vec{n}) = \arctan\left(\frac{n_2}{n_1}\right).$$



Frank diagram



“Wulff shape”

Anisotropic surface energy

$$|\Gamma|_\gamma = \int_\Gamma \hat{\gamma}(\vec{\nu}) \, ds = \int_\Gamma \gamma(\vec{\nu}) \, ds$$

where $\gamma : \mathbb{R}^2 \rightarrow \mathbb{R}_{\geq 0}$ is absolutely homogeneous of degree one, i.e.

$$\gamma(\lambda \vec{\rho}) = |\lambda| \gamma(\vec{\rho}) \quad \forall \vec{\rho} \in \mathbb{R}^2, \quad \forall \lambda \in \mathbb{R}.$$

Let $\Gamma(\varepsilon) := \{\vec{z} + \varepsilon \vec{g}(\vec{z}) : \vec{z} \in \Gamma\}$. First variation of this energy yields

$$\frac{d}{d\varepsilon} |\Gamma(\varepsilon)|_\gamma \Big|_{\varepsilon=0} = - \int_\Gamma \vec{\kappa}_\gamma \cdot \vec{g} \, ds;$$

where

$$\vec{\kappa}_\gamma = \kappa_\gamma \vec{\nu} = [\gamma'(\vec{\nu})]_s^\perp$$

is the anisotropic mean curvature vector, and $\vec{\nu} = -\vec{\kappa}_s^\perp$.

In the isotropic case, $\gamma(\vec{\rho}) = |\vec{\rho}|$, we have that $|\Gamma|_\gamma \equiv |\Gamma|$, $\vec{\kappa}_\gamma \equiv \vec{\kappa}$ and $\kappa_\gamma \equiv \kappa$.

Anisotropic surface diffusion in the plane

This leads to the geometric evolution equation

$$\text{Anisotropic surface diffusion: } \mathcal{V} = -[\kappa_\gamma]_{ss}.$$

Similarly to the isotropic case, $\gamma(\vec{\rho}) = |\vec{\rho}|$, we have that

$$\frac{d}{dt} |\Gamma(t)|_\gamma = - \int_{\Gamma(t)} \mathcal{V} \kappa_\gamma ds = - \int_{\Gamma(t)} ([\kappa_\gamma]_s)^2 ds$$

and

$$\frac{d}{dt} |D(t)| = \int_{\Gamma(t)} \mathcal{V} ds = - \int_{\Gamma(t)} [\kappa_\gamma]_{ss} ds = 0.$$

It is also possible to introduce an anisotropic mobility $\beta : \mathbb{S}^{d-1} \rightarrow \mathbb{R}_{>0}$ and then consider the more general flow

$$\mathcal{V} = -(\beta(\vec{\nu}) [\kappa_\gamma]_s)_s.$$

For simplicity, we fix $\beta = 1$ throughout.

Weak formulation

For smooth test functions $\varphi \in V = H^1(\mathbb{R}/\mathbb{Z}; \mathbb{R})$ and $\vec{\varphi} \in \underline{V} = H^1(\mathbb{R}/\mathbb{Z}; \mathbb{R}^2)$ it holds that

$$\int_{\Gamma} \vec{x}_t \cdot \vec{\nu} \varphi \, ds = \int_{\Gamma} [\chi_{\gamma}]_s \varphi_s \, ds,$$
$$\int_{\Gamma} \chi_{\gamma} \vec{\nu} \cdot \vec{\varphi} \, ds + \int_{\Gamma} \gamma'(\vec{x}_s^{\perp}) \cdot \vec{\varphi}_s^{\perp} \, ds = 0.$$

For a general anisotropy, it does not appear possible to approximate the term

$$\int_{\Gamma} \gamma'(\vec{x}_s^{\perp}) \cdot \vec{\varphi}_s^{\perp} \, ds$$

on say, Γ^m , in terms of $\vec{\nu}^m$ and \vec{X}^{m+1} , such that the overall finite element approximation is unconditionally stable.

BGN class of anisotropies

The desired stability properties lead us to consider sums of weighted norms. They allow us to model a wide variety of anisotropies, including crystalline surface energy densities.

In particular, from now on we consider anisotropies of the form

$$\gamma(\vec{p}) = \sum_{\ell=1}^L \gamma_{\ell}(\vec{p}), \quad \gamma_{\ell}(\vec{p}) = [\vec{p} \cdot G_{\ell} \vec{p}]^{\frac{1}{2}}, \quad \forall \vec{p} \in \mathbb{R}^2,$$

where $G_{\ell} \in \mathbb{R}^{2 \times 2}$, for $\ell = 1, \dots, L$, are symmetric and positive definite matrices.

This class of anisotropies was first proposed in Barrett, Garcke & Nürnberg (2008). Hence we call an anisotropy of the above form a *BGN anisotropy*.

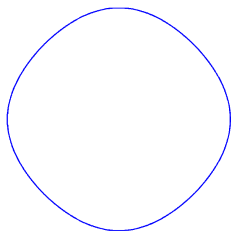
For later use we note that

$$\gamma'(\vec{p}) = \sum_{\ell=1}^L [\gamma_{\ell}(\vec{p})]^{-1} G_{\ell} \vec{p} \quad \forall \vec{p} \in \mathbb{R}^2 \setminus \{\vec{0}\}.$$

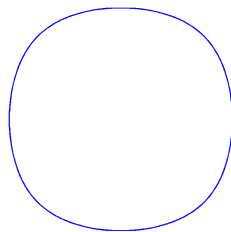
BGN Anisotropies

Examples

Regularized l^1 -norm:
$$\gamma(\vec{p}) = \sum_{\ell=1}^2 [\delta^2 |\vec{p}|^2 + p_{\ell}^2(1 - \delta^2)]^{\frac{1}{2}}, \quad \delta = \frac{1}{2}.$$



Frank diagram

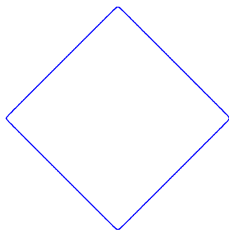


Wulff shape

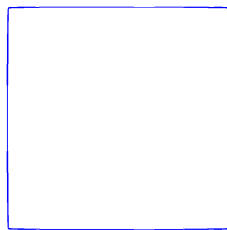
BGN Anisotropies

Examples

Regularized l^1 -norm:
$$\gamma(\vec{p}) = \sum_{\ell=1}^2 [\delta^2 |\vec{p}|^2 + p_{\ell}^2(1 - \delta^2)]^{\frac{1}{2}}, \quad \delta = 0.01.$$



Frank diagram

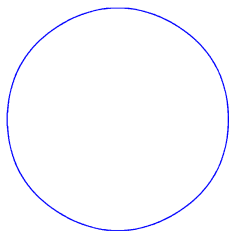


Wulff shape

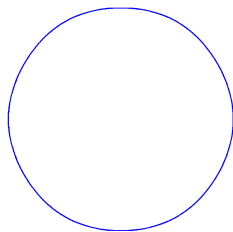
BGN Anisotropies

Examples

Hexagonal anisotropy: $\gamma(\vec{p}) = \sum_{\ell=1}^3 \left[\vec{p} \cdot R_{\ell}^T \begin{pmatrix} 1 & 0 \\ 0 & \delta^2 \end{pmatrix} R_{\ell} \vec{p} \right]^{\frac{1}{2}}, \quad \delta = \frac{1}{2}.$



Frank diagram

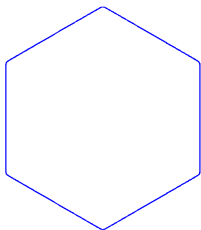


Wulff shape

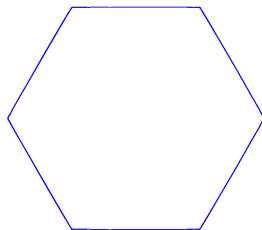
BGN Anisotropies

Examples

Hexagonal anisotropy:
$$\gamma(\vec{p}) = \sum_{\ell=1}^3 \left[\vec{p} \cdot R_{\ell}^T \begin{pmatrix} 1 & 0 \\ 0 & \delta^2 \end{pmatrix} R_{\ell} \vec{p} \right]^{\frac{1}{2}}, \quad \delta = 0.01.$$



Frank diagram



Wulff shape

Parametric finite element approximation

Recall

$$\int_{\Gamma} \vec{x}_t \cdot \vec{\nu} \varphi \, ds = \int_{\Gamma} [\kappa_{\gamma}]_s \cdot \varphi_s \, ds, \quad \int_{\Gamma} \kappa_{\gamma} \vec{\nu} \cdot \vec{\varphi} \, ds + \int_{\Gamma} \gamma'(\vec{x}_s^{\perp}) \cdot \vec{\varphi}_s^{\perp} \, ds = 0,$$

$$\text{where } \gamma'(\vec{x}_s^{\perp}) = \sum_{\ell=1}^L [\gamma_{\ell}(\vec{x}_s^{\perp})]^{-1} G_{\ell} \vec{x}_s^{\perp} = \sum_{\ell=1}^L [\gamma_{\ell}(\vec{\nu})]^{-1} G_{\ell} \vec{x}_s^{\perp}.$$

(\mathcal{P}_{γ}^h) Find $(\vec{X}^{m+1}, \kappa_{\gamma}^{m+1}) \in \underline{V}^h \times V^h$ such that

$$\left\langle \frac{\vec{X}^{m+1} - \vec{X}^m}{\tau_m}, \chi \vec{\nu}^m \right\rangle_{\Gamma^m}^h - \langle [\kappa_{\gamma}^{m+1}]_s, \chi_s \rangle_{\Gamma^m} = 0 \quad \forall \chi \in V^h,$$

$$\langle \kappa_{\gamma}^{m+1} \vec{\nu}^m, \vec{\eta} \rangle_{\Gamma^m}^h + \sum_{\ell=1}^L \langle [\gamma^{(\ell)}(\vec{\nu}^m)]^{-1} G^{(\ell)} [\vec{X}_s^{m+1}]^{\perp}, \vec{\eta}_s^{\perp} \rangle_{\Gamma^m} = 0 \quad \forall \vec{\eta} \in \underline{V}^h.$$

Note that for $\gamma(\vec{\rho}) = |\vec{\rho}|$ the scheme (\mathcal{P}_{γ}^h) collapses to the isotropic scheme (\mathcal{P}_0^h) discussed earlier.

Existence, uniqueness and stability

- **Existence, Uniqueness**

The scheme is linear. So under mild assumptions on \vec{X}^m , there exists a unique solution $(\vec{X}^{m+1}, \kappa_\gamma^{m+1}) \in \underline{V}^h \times V^h$ to (\mathcal{P}_γ^h) .

- **Stability** For all $k = 1 \rightarrow M$ it holds that

$$|\Gamma^k|_\gamma + \sum_{m=0}^{k-1} \tau_m \langle [\kappa_\gamma^{m+1}]_s, [\kappa_\gamma^{m+1}]_s \rangle_{\Gamma^m} \leq |\Gamma^0|_\gamma.$$

- **Area conservation** for a continuous in time semidiscrete scheme.
- **Equidistribution of mesh points** for $\vec{X}(t)$, where $\vec{X}(t)$ not locally parallel, for any $t > 0$, for a continuous in time semidiscrete scheme, with respect to a non-trivial **anisotropic weighting function**.

Tangential Movement

$$\gamma(\vec{p}) = \sqrt{p_1^2 + 0.1 p_2^2}$$

\Rightarrow

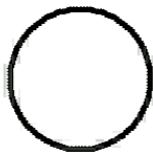
Wulff shape is $\sqrt{10} : 1$ ellipse



$$\gamma(\vec{p}) = \sqrt{p_1^2 + 0.01 p_2^2}$$

\Rightarrow

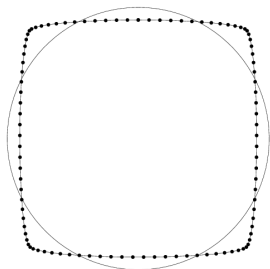
Wulff shape is $10 : 1$ ellipse



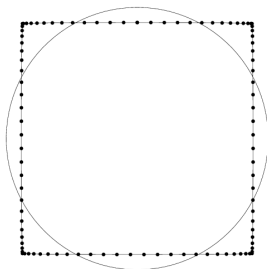
Numerical results

Regularized l^1 -norm:
$$\gamma(\vec{p}) = \sum_{\ell=1}^2 [\delta^2 |\vec{p}|^2 + p_\ell^2(1 - \delta^2)]^{\frac{1}{2}} .$$

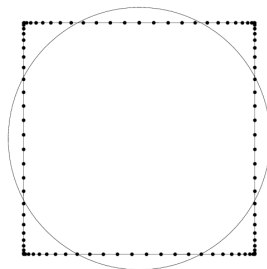
$$\delta = 10^{-1}$$



$$\delta = 10^{-2}$$

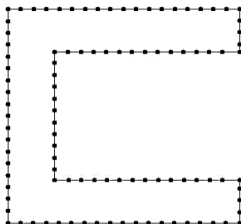


$$\delta = 10^{-3}$$



Crystalline surface diffusion

$$\gamma(\vec{p}) = \sum_{\ell=1}^2 \sqrt{10^{-5} |\vec{p}|^2 + p_{\ell}^2 (1 - 10^{-5})} \quad \Rightarrow \quad \mathcal{W} \text{ is close to a square}$$

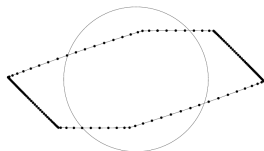
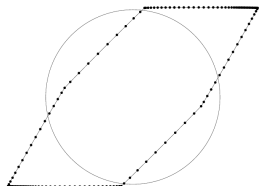
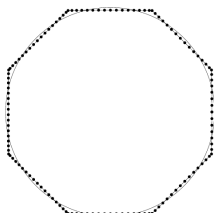
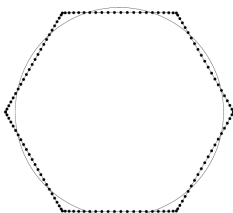
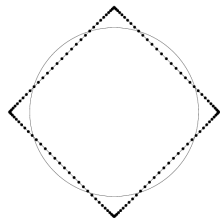


New facets appear in evolution.

Other crystalline shapes

$$\gamma(\vec{p}) = \sum_{\ell=1}^L \left[\vec{p} \cdot R^T(\theta_\ell) \begin{pmatrix} 1 & 0 \\ 0 & \delta^2 \end{pmatrix} R(\theta_\ell) \vec{p} \right]^{\frac{1}{2}}, \quad \delta = 0.01.$$

$$(\theta_1, \dots, \theta_L) = \left(\frac{\pi}{4}, \frac{3\pi}{4} \right), \left(0, \frac{\pi}{3}, \frac{2\pi}{3} \right), \left(0, \frac{\pi}{4}, \frac{\pi}{2}, \frac{3\pi}{4} \right), \left(0, \frac{\pi}{4}, \frac{\pi}{3} \right), \left(0, \frac{\pi}{10}, \frac{\pi}{9}, \frac{3\pi}{4} \right).$$



Isotropic surface diffusion in 3d

Family of evolving hypersurfaces $(\Gamma(t))_{t \in [0, T]}$, without boundary.

$$\mathcal{V} = -\Delta_S \kappa \quad \text{on } \Gamma(t),$$

where $\Delta_S = \nabla_S \cdot \nabla_S$ is the Laplace–Beltrami operator on $\Gamma(t)$, with ∇_S and ∇_S denoting the surface divergence and the surface gradient operators.

As before we have

$$\frac{d}{dt} |\Gamma(t)| = - \int_{\Gamma(t)} \mathcal{V} \kappa \, ds = - \int_{\Gamma(t)} |\nabla_S \kappa|^2 \, ds \equiv -\|\mathcal{V}\|_{H^{-1}(\Gamma(t))}^2 \leq 0$$

and

$$\frac{d}{dt} |D(t)| = \int_{\Gamma(t)} \mathcal{V} \, ds = - \int_{\Gamma(t)} \Delta_S \kappa \, ds = 0.$$

BGN formulation:

$$\vec{x}_t \cdot \vec{\nu} = -\Delta_S \kappa, \quad \kappa \vec{\nu} = \Delta_S \vec{x} \quad \text{on } \Gamma(t).$$

Parametric finite element approximation

(\mathcal{P}^h) Find $(\vec{X}^{m+1}, \kappa^{m+1}) \in \underline{V}^h(\Gamma(m)) \times V^h(\Gamma^m)$ such that

$$\left\langle \frac{\vec{X}^{m+1} - \vec{X}^m}{\tau_m}, \chi \vec{\nu}^m \right\rangle_{\Gamma^m}^h - \langle \nabla_s \kappa^{m+1}, \nabla_s \chi \rangle_{\Gamma^m} = 0 \quad \forall \chi \in V^h(\Gamma^m),$$
$$\langle \kappa^{m+1} \vec{\nu}^m, \vec{\eta} \rangle_{\Gamma^m}^h + \langle \nabla_s \vec{X}^{m+1}, \nabla_s \vec{\eta} \rangle_{\Gamma^m} = 0 \quad \forall \vec{\eta} \in \underline{V}^h(\Gamma^m).$$

- **Existence, Uniqueness**

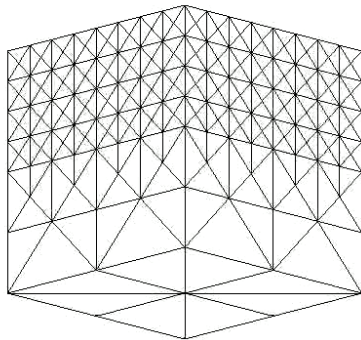
Under mild assumptions on \vec{X}^m , $\exists!$ $(\vec{X}^{m+1}, \kappa^{m+1}) \in \underline{V}^h \times V^h$.

- **Stability** For all $k = 1 \rightarrow M$ it holds that

$$|\Gamma^k| + \sum_{m=0}^{k-1} \tau_m \langle \nabla_s \kappa^{m+1}, \nabla_s \kappa^{m+1} \rangle_{\Gamma^m} \leq |\Gamma^0|.$$

- **Volume conservation** for a continuous in time semidiscrete scheme.
- **Good mesh properties.**

Tangential distribution of mesh points

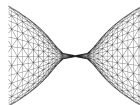
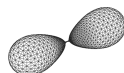
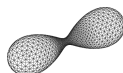
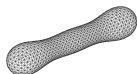
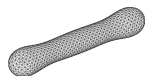
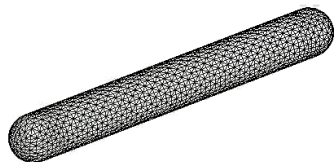


No heuristical redistribution necessary.

Numerical results

Surface Diffusion leading to pinch-off.

Rounded cylinder $8 \times 1 \times 1$.



Anisotropic surface diffusion in 3d

$$\mathcal{V} = -\Delta_s \kappa_\gamma \quad \text{on } \Gamma(t),$$

where κ_γ is the anisotropic mean curvature, defined as before via the first variation of the anisotropic surface energy $|\Gamma|_\gamma = \int_\Gamma \gamma(\vec{\nu}) \, ds$. In particular, it holds that

$$\frac{d}{d\varepsilon} |\Gamma(\varepsilon)|_\gamma \Big|_{\varepsilon=0} = - \int_\Gamma \vec{\kappa}_\gamma \cdot \vec{g} \, ds;$$

where

$$\vec{\kappa}_\gamma = \kappa_\gamma \vec{\nu}, \quad \kappa_\gamma = -\nabla_s \cdot \vec{\nu}_\gamma, \quad \vec{\nu}_\gamma = \gamma'(\vec{\nu}).$$

As before we have

$$\frac{d}{dt} |\Gamma(t)|_\gamma = - \int_{\Gamma(t)} \mathcal{V} \kappa_\gamma \, ds = - \int_{\Gamma(t)} |\nabla_s \kappa_\gamma|^2 \, ds \equiv -\|\mathcal{V}\|_{H^{-1}(\Gamma(t))}^2 \leq 0$$

and

$$\frac{d}{dt} |D(t)| = \int_{\Gamma(t)} \mathcal{V} \, ds = - \int_{\Gamma(t)} \Delta_s \kappa_\gamma \, ds = 0.$$

Variational formulation of anisotropic curvature

Prior to BGN (2008), all parametric approaches to anisotropic geometric evolution equations were based on the identity

$$\begin{aligned}\vec{\kappa}_\gamma &= \kappa_\gamma \vec{\nu} = -[\nabla_s \gamma'(\vec{\nu})] \vec{\nu} \\ &= -\nabla_s \cdot (\vec{\nu} [\gamma'(\vec{\nu})]^T) + \nabla_s \cdot (\gamma(\vec{\nu}) \nabla_s \vec{x}) - \gamma(\vec{\nu}) \Delta_s \vec{x}.\end{aligned}$$

The above identity uses *isotropic* differential operators, and does not lead to stable schemes upon discretization.

Key idea: Use *anisotropic* differential operators that are induced by the metrics that make up the BGN anisotropy γ .

Recall that in 2d we had:

$$\int_\Gamma \kappa_\gamma \vec{\nu} \cdot \vec{\varphi} \, ds = - \sum_{\ell=1}^L \int_\Gamma [\gamma_\ell(\vec{\nu})]^{-1} G_\ell \vec{x}_s^\perp \cdot \vec{\varphi}_s^\perp \, ds \quad \forall \vec{\varphi} \in \underline{V},$$

which can be viewed as involving inner products between “anisotropic surface gradients”.

Currently, for $d = 2$ or $d = 3$, we consider the class of BGN anisotropies

$$\gamma(\vec{p}) = \sum_{\ell=1}^L \gamma_{\ell}(\vec{p}), \quad \gamma_{\ell}(\vec{p}) = [\vec{p} \cdot G_{\ell} \vec{p}]^{\frac{1}{2}}, \quad \forall \vec{p} \in \mathbb{R}^d,$$

where $G_{\ell} \in \mathbb{R}^{d \times d}$, for $\ell = 1, \dots, L$, are symmetric and positive definite matrices.

In 2d, it turns out that the above class of anisotropies is rich enough to (approximatively) model any even, convex anisotropy.

However, in 3d this is not the case. For example, in the crystalline limit, the above class always leads to parallel opposing facets in the Wulff shape.

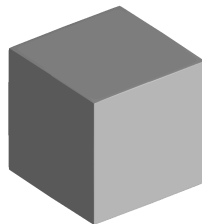
BGN Anisotropies

Examples

Regularized l^1 -norm:
$$\gamma(\vec{p}) = \sum_{\ell=1}^3 [\delta^2 |\vec{p}|^2 + p_{\ell}^2(1 - \delta^2)]^{\frac{1}{2}}, \quad \delta = 0.01.$$



Frank diagram



Wulff shape

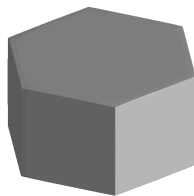
BGN Anisotropies

Examples

Hexagonal anisotropy: $\gamma(\vec{p}) = \sum_{\ell=1}^4 \left[\vec{p} \cdot R_{\ell}^T \text{diag}(1, \delta^2, \delta^2) R_{\ell} \vec{p} \right]^{\frac{1}{2}}, \delta = 0.01.$



Frank diagram

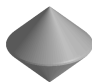


Wulff shape

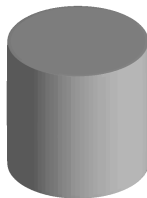
BGN Anisotropies

Examples

$$\text{Cylindrical anisotropy: } \gamma(\vec{p}) = [\vec{p} \cdot \text{diag}(\delta^2, \delta^2, 1) \vec{p}]^{\frac{1}{2}} + [\vec{p} \cdot \text{diag}(1, 1, \delta^2) \vec{p}]^{\frac{1}{2}},$$
$$\delta = 0.01.$$



Frank diagram



Wulff shape

BGN Anisotropies

It turns out that on considering the l^r -norm of weighted norms it is possible to model a large class of even, convex anisotropies in 3d.

In particular, for $r \geq 1$, we consider

$$\gamma(\vec{p}) = \left[\sum_{\ell=1}^L [\gamma_{\ell}(\vec{p})]^r \right]^{\frac{1}{r}}, \quad \gamma_{\ell}(\vec{p}) = [\vec{p} \cdot G_{\ell} \vec{p}]^{\frac{1}{2}}, \quad \forall \vec{p} \in \mathbb{R}^d.$$

This class of anisotropies was first proposed in Barrett, Garcke & Nürnberg (2008). We call an anisotropy of the above form an *r-BGN anisotropy*.

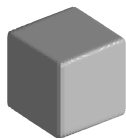
For later use we note that

$$\gamma'(\vec{p}) = \sum_{\ell=1}^L \left[\frac{\gamma_{\ell}(\vec{p})}{\gamma(\vec{p})} \right]^{r-1} \gamma'_{\ell}(\vec{p}) \quad \forall \vec{p} \in \mathbb{R}^d \setminus \{\vec{0}\}.$$

BGN Anisotropies

Example

$$\text{Cubic anisotropy: } \gamma(\vec{p}) = \left[\sum_{\ell=1}^3 [\delta^2 |\vec{p}|^2 + p_\ell^2 (1 - \delta^2)]^{\frac{r}{2}} \right]^{\frac{1}{r}}, \quad \delta = 0.01, r = 30.$$



Frank diagram



Wulff shape

Variational formulation of anisotropic curvature

Let $G \in \mathbb{R}^{3 \times 3}$ be symmetric and positive definite. Let $\tilde{G} = [\det G]^{\frac{1}{2}} G^{-1}$, and let $(\cdot, \cdot)_{\tilde{G}}$ be the inner product on \mathbb{R}^3 induced by \tilde{G} .

At a point $\vec{z} \in \Gamma$, let $\{\vec{t}_1, \vec{t}_2\}$ be an orthonormal basis of the tangent space $T_{\vec{z}}\Gamma$ with respect to the inner product $(\cdot, \cdot)_{\tilde{G}}$.

Then for $g : \Gamma \rightarrow \mathbb{R}$ we define the anisotropic surface gradient

$$(\nabla_s^{\tilde{G}} g)(\vec{z}) := \sum_{i=1}^2 (\partial_{\vec{t}_i} g)(\vec{z}) \vec{t}_i.$$

Similarly, for $\vec{g} : \Gamma \rightarrow \mathbb{R}^2$ we define the anisotropic surface divergence

$$(\nabla_s^{\tilde{G}} \cdot \vec{g})(\vec{z}) := \sum_{i=1}^2 (\partial_{\vec{t}_i} \vec{g})(\vec{z}) \cdot \tilde{G} \vec{t}_i$$

and the anisotropic surface gradient

$$(\nabla_s^{\tilde{G}} \vec{g})(\vec{z}) := \sum_{i=1}^2 (\partial_{\vec{t}_i} \vec{g})(\vec{z}) \otimes \tilde{G} \vec{t}_i.$$

Variational formulation of anisotropic curvature

Finally, we also define the inner product

$$(\nabla_s^{\tilde{G}} \vec{u}, \nabla_s^{\tilde{G}} \vec{v})_{\tilde{G}} := \sum_{i=1}^2 (\partial_{\tilde{t}_i} \vec{u}, \partial_{\tilde{t}_i} \vec{v})_{\tilde{G}}.$$

Then it can be shown for the r -BGN anisotropy that

$$\kappa_\gamma \vec{v} = \sum_{\ell=1}^L \gamma_\ell(\vec{v}) \tilde{G}_\ell \nabla_s^{\tilde{G}_\ell} \cdot \left[\left[\frac{\gamma_\ell(\vec{v})}{\gamma(\vec{v})} \right]^{r-1} \nabla_s^{\tilde{G}_\ell} \vec{x} \right],$$

which implies the weak form

$$\int_\Gamma \kappa_\gamma \vec{v} \cdot \vec{\varphi} \, ds + \sum_{\ell=1}^L \int_\Gamma \left[\frac{\gamma_\ell(\vec{v})}{\gamma(\vec{v})} \right]^{r-1} (\nabla_s^{\tilde{G}_\ell} \vec{x}, \nabla_s^{\tilde{G}_\ell} \vec{\varphi})_{\tilde{G}_\ell} \gamma_\ell(\vec{v}) \, ds = 0$$

for all $\vec{\varphi} \in [H^1(\Gamma)]^3$.

Parametric finite element approximation

(\mathcal{P}^h) Find $(\vec{X}^{m+1}, \kappa_\gamma^{m+1}) \in \underline{V}^h(\Gamma^m) \times V^h(\Gamma^m)$ such that

$$\left\langle \frac{\vec{X}^{m+1} - \vec{X}^m}{\tau_m}, \chi \vec{\nu}^m \right\rangle_{\Gamma^m}^h - \langle \nabla_s \kappa_\gamma^{m+1}, \nabla_s \chi \rangle_{\Gamma^m} = 0 \quad \forall \chi \in V^h(\Gamma^m),$$
$$\langle \kappa_\gamma^{m+1} \vec{\nu}^m, \vec{\eta} \rangle_{\Gamma^m}^h + \sum_{\ell=1}^L \int_{\Gamma^m} \left[\frac{\gamma_\ell(\vec{\nu}^{m+1})}{\gamma(\vec{\nu}^{m+1})} \right]^{r-1} (\nabla_s^{\tilde{G}_\ell} \vec{X}^{m+1}, \nabla_s^{\tilde{G}_\ell} \vec{\eta})_{\tilde{G}_\ell} \gamma_\ell(\vec{\nu}^m) ds$$
$$= 0 \quad \forall \vec{\eta} \in \underline{V}^h(\Gamma^m).$$

$r = 1$: Linear system. Existence, uniqueness and unconditional stability.

$r > 1$: Nonlinear system. Unconditional Stability.

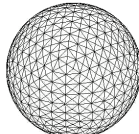
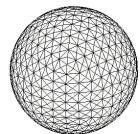
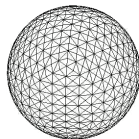
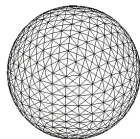
Numerical results

Cube ($r = 1$, $L = 3$),

Hexagonal Prism ($r = 1$, $L = 4$),

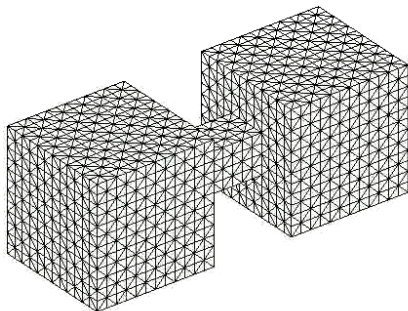
Octahedron ($r = 30$, $L = 3$),

Cylinder Wulff Shape ($r = 1$, $L = 2$).



Numerical results

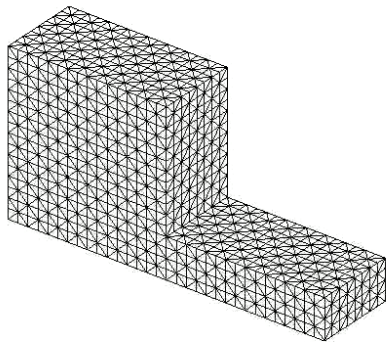
Cubic Wulff shape ($r = 1$, $L = 3$)



Dumbbell

Numerical results

Cubic Wulff shape ($r = 1$, $L = 3$)



Facet breaking

The presented treatment of the anisotropy in the parametric framework easily extends to other applications.

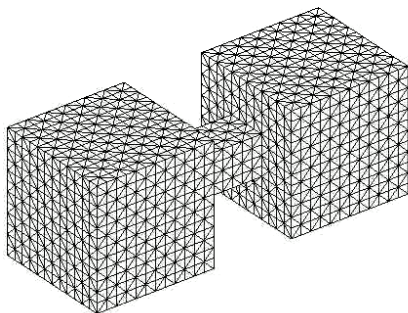
- Anisotropic mean curvature flow: $\mathcal{V} = \kappa_\gamma$.
- Anisotropic mean curvature flow and surface diffusion of curve networks and surface clusters.
- Anisotropic Stefan problems, including applications to snow crystal growth.

Numerical results

Anisotropic mean curvature flow

$$\mathcal{V} = \kappa_\gamma$$

Cubic Wulff shape ($r = 1$, $L = 3$)

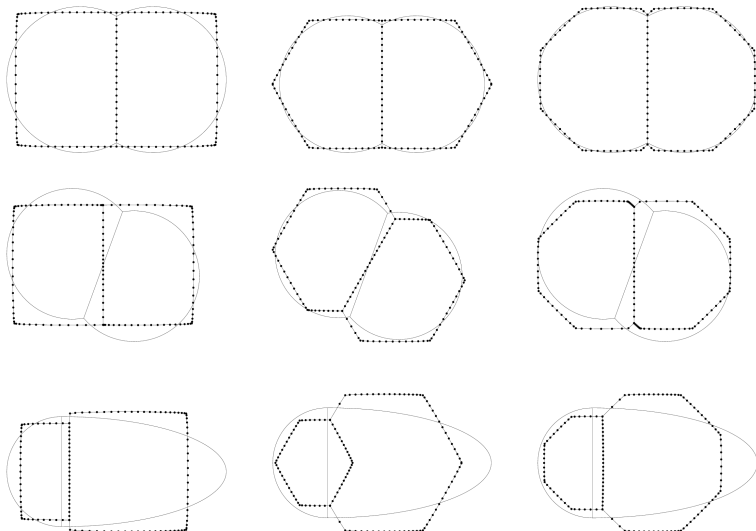


Dumbbell leading to pinch-off.

Numerical results

Anisotropic surface diffusion for curve networks

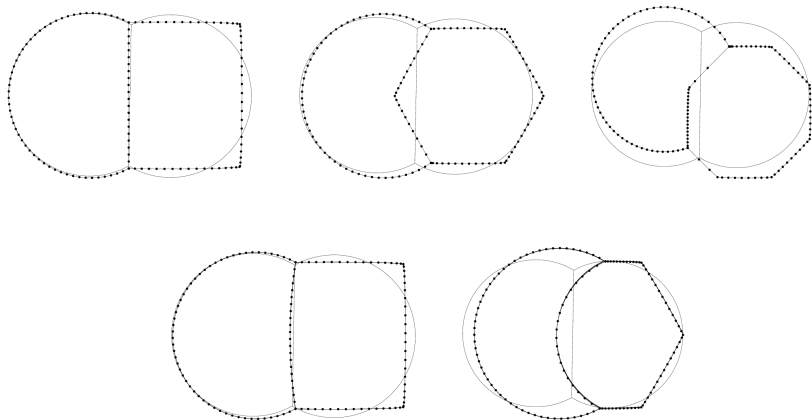
$$\mathcal{V} = -[\chi_\gamma]_{ss} + \text{triple junction conditions}$$



Numerical results

Anisotropic surface diffusion for curve networks

$$\mathcal{V} = -[\chi_\gamma]_{SS} + \text{triple junction conditions}$$

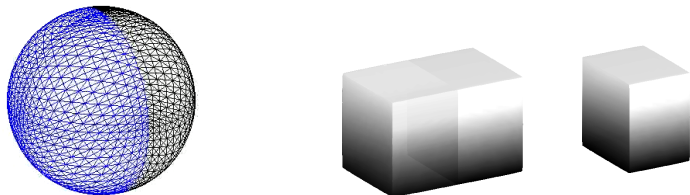


Anisotropic double bubbles.

Numerical results

Anisotropic surface diffusion for surface clusters

$$\mathcal{V} = -\Delta_s \kappa_\gamma + \text{triple junction conditions}$$

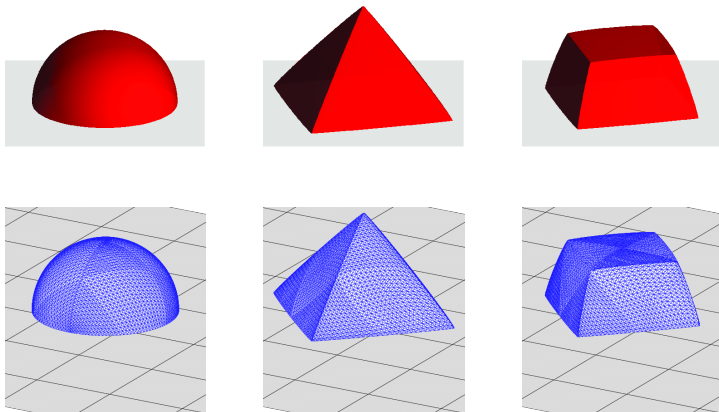


Anisotropic double bubble.

Numerical results

Anisotropic surface diffusion for surface clusters

$$\mathcal{V} = -\Delta_s \mathcal{H}_\gamma + \text{boundary conditions}$$



Isotropic and anisotropic equilibrium shapes.

Numerical results

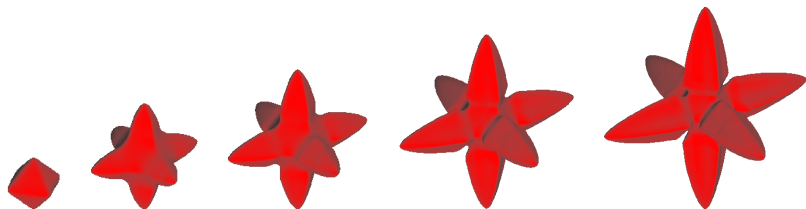
Anisotropic Stefan problem with kinetic undercooling

Find the temperature $u(\cdot, t) : \Omega \rightarrow \mathbb{R}$ and the interface $\Gamma(t) \subset \Omega$ such that for $t \in (0, T]$

$$\vartheta u_t - \mathcal{K} \Delta u = 0 \quad \text{in } \Omega \setminus \Gamma(t),$$

$$\left[\mathcal{K} \frac{\partial u}{\partial \vec{\nu}} \right]_{\Gamma(t)} = -\lambda \mathcal{V} \quad \text{on } \Gamma(t),$$

$$\rho \mathcal{V} = \alpha \kappa_\gamma - a u \quad \text{on } \Gamma(t).$$



Numerical results

Snow crystal growth

o

o

Phase field approximations

Isotropic Cahn–Hilliard equation

The following degenerate Cahn–Hilliard equation is a phase field model for isotropic surface diffusion.

$$\begin{aligned}\varepsilon u_t &= \nabla \cdot (b(u) \nabla w) && \text{in } \Omega_T = \Omega \times [0, T], \\ w &= -\varepsilon \Delta u + \varepsilon^{-1} \Psi'(u) && \text{in } \Omega_T.\end{aligned}$$

For example, $b(s) = (1 - s^2)^2$ and $\Psi(s) = \frac{1}{4} (1 - s^2)^2$, or $b(s) = 1 - s^2$ and Ψ is the obstacle potential: $\Psi(s) = \begin{cases} \frac{1}{2}(1 - s^2) & s \in [-1, 1], \\ \infty & s \notin [-1, 1]. \end{cases}$

As $\varepsilon \rightarrow 0$, the zero-level sets of u move by surface diffusion: $\sigma_\Psi \mathcal{V} = -\Delta_s \mathcal{V}$.

See e.g. Lee, Münch & Süli (2016).

Phase field approximations

Isotropic Cahn–Hilliard equation

A possible semi-implicit finite element approximation, based on a mixed formulation, using piecewise linear finite elements, is given as follows.

Find $(U^{n+1}, W^{n+1}) \in S^h(\Omega) \times S^h(\Omega)$ such that, for all $\eta, \chi \in S^h(\Omega)$,

$$\begin{aligned} \varepsilon \left(\frac{U^{n+1} - U^n}{\Delta t}, \eta \right)^h + (b(U^n) \nabla W^{n+1}, \nabla \eta)^h &= 0, \\ \varepsilon (\nabla U^{n+1}, \nabla \chi) + \varepsilon^{-1} (\Psi'_+(U^{n+1}) + \Psi'_-(U^n), \chi)^h &= (W^{n+1}, \chi)^h. \end{aligned}$$

Here (\cdot, \cdot) and $(\cdot, \cdot)^h$ are the standard and mass-lumped L^2 -inner products on Ω , respectively.

Moreover, the splitting $\Psi = \Psi_+ + \Psi_-$ is such that Ψ_+ is convex, and Ψ_- is concave.

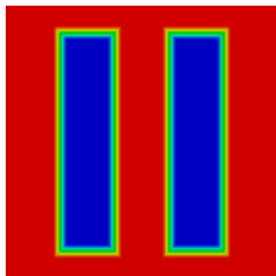
Nonlinear system. Existence, uniqueness and unconditional stability.

Phase field approximations

Isotropic Cahn–Hilliard equation

Phase field approximations replace the sharp interface Γ with a diffuse interfacial layer, $\{|u| < 1\}$.

This allows the application of standard PDE solution techniques, and topological changes are trivially captured.



Topological change.

Phase field approximations

Anisotropic Cahn–Hilliard equation

The following degenerate Cahn–Hilliard equation is a phase field model for anisotropic surface diffusion, for a given anisotropy function γ .

$$\begin{aligned}\varepsilon u_t &= \nabla \cdot (b(u) \nabla w) && \text{in } \Omega_T, \\ w &= -\varepsilon \nabla \cdot (\gamma(\nabla u) \gamma'(\nabla u)) + \varepsilon^{-1} \psi'(u) && \text{in } \Omega_T.\end{aligned}$$

As $\varepsilon \rightarrow 0$, the zero-level sets of u move by surface diffusion: $\sigma_{\Psi \mathcal{V}} = -\Delta_s \kappa_\gamma$.

For a general anisotropy, the discretization of the nonlinear term

$$\nabla \cdot (\gamma(\nabla u) \gamma'(\nabla u))$$

is highly nontrivial, with stability and efficient solvability being the main challenges.

However, for an r -BGN anisotropy, we can introduce a natural linearization that leads to an unconditionally stable finite element approximation.

Phase field approximations

BGN Anisotropies

Recall that

$$\gamma(\vec{p}) \gamma'(\vec{p}) = \gamma(\vec{p}) \sum_{\ell=1}^L \left[\frac{\gamma_{\ell}(\vec{p})}{\gamma(\vec{p})} \right]^{r-1} [\gamma_{\ell}(\vec{p})]^{-1} G_{\ell} \vec{p} \quad \forall \vec{p} \in \mathbb{R}^d \setminus \{\vec{0}\}.$$

Given a \vec{q} close to \vec{p} , we now “linearize” $\gamma(\vec{p}) \gamma'(\vec{p})$ by $B_r(\vec{q}, \vec{p}) \vec{p}$, where

$$B_r(\vec{q}, \vec{p}) := \begin{cases} \gamma(\vec{q}) \sum_{\ell=1}^L \left[\frac{\gamma_{\ell}(\vec{p})}{\gamma(\vec{p})} \right]^{r-1} [\gamma_{\ell}(\vec{q})]^{-1} G_{\ell} & \vec{q} \neq \vec{0}, \\ L^{\frac{1}{r}} \sum_{\ell=1}^L \left[\frac{\gamma_{\ell}(\vec{p})}{\gamma(\vec{p})} \right]^{r-1} G_{\ell} & \vec{q} = \vec{0}, \end{cases} \quad \forall \vec{p} \in \mathbb{R}^d.$$

Clearly it holds that $\lim_{\vec{q} \rightarrow \vec{p}} B_r(\vec{q}, \vec{p}) \vec{p} = \gamma(\vec{p}) \gamma'(\vec{p})$ for all $\vec{p} \in \mathbb{R}^d$.

In addition, $B_r(\vec{q}, \vec{p})$ is symmetric, positive definite for all $\vec{q}, \vec{p} \in \mathbb{R}^d$.

Phase field approximations

Anisotropic Cahn–Hilliard equation

Find $(U^{n+1}, W^{n+1}) \in S^h(\Omega) \times S^h(\Omega)$ such that, for all $\eta, \chi \in S^h(\Omega)$,

$$\varepsilon \left(\frac{U^{n+1} - U^n}{\Delta t}, \eta \right)^h + (b(U^n) \nabla W^{n+1}, \nabla \eta)^h = 0,$$

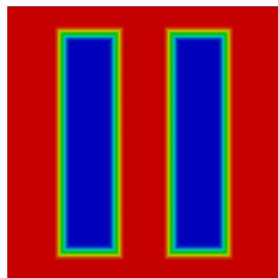
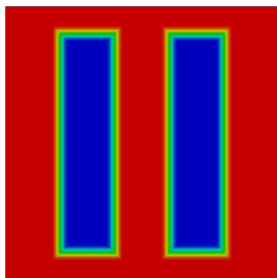
$$\varepsilon (B_r(\nabla U^n, \nabla U^{n+1}) \nabla U^{n+1}, \nabla \chi) \\ + \varepsilon^{-1} (\Psi'_+(U^{n+1}) + \Psi'_-(U^n), \chi)^h = (W^{n+1}, \chi)^h.$$

$r = 1$: Nonlinear system, as nonlinear as in the isotropic case.
Existence, uniqueness and unconditional stability.

$r > 1$: Highly nonlinear system. Unconditional stability.

Numerical results

Anisotropic Cahn–Hilliard equation



Other applications

The presented treatment of the anisotropy in the phase field framework easily extends to other applications.

- Anisotropic Allen–Cahn equation:

$$\varepsilon \varphi_t = \varepsilon \nabla \cdot (\gamma(\nabla \varphi) \gamma'(\nabla \varphi)) - \varepsilon^{-1} \Psi'(\varphi).$$

(as a phase field model for anisotropic mean curvature flow)

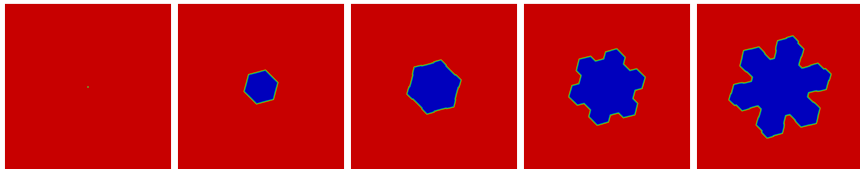
- General anisotropic phase field equations:

$$\begin{aligned} \vartheta w_t + \frac{1}{2} \lambda \varphi_t - \mathcal{K} \Delta w &= 0, \\ \frac{1}{2} \sigma_\Psi a w &= \rho \varepsilon \varphi_t - \alpha \varepsilon \nabla \cdot (\gamma(\nabla \varphi) \gamma'(\nabla \varphi)) + \alpha \varepsilon^{-1} \Psi'(\varphi). \end{aligned}$$

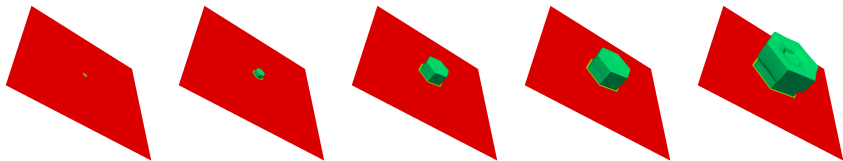
(as a phase field model for anisotropic Stefan problems)

Numerical results

Anisotropic phase field model



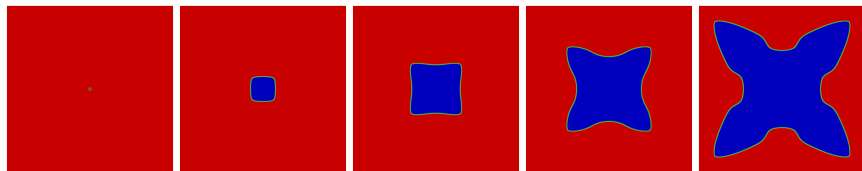
Ice crystal growth in 2d.



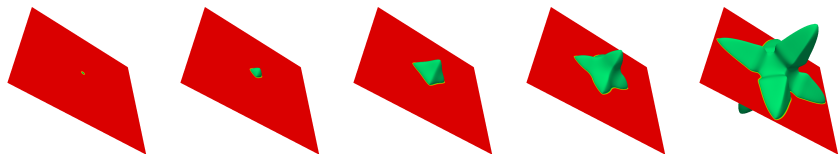
Ice crystal growth in 3d.

Numerical results

Anisotropic phase field model



Dendritic growth in 2d.



Dendritic growth in 3d.

- J. W. Barrett, H. Garcke, and R. Nürnberg, *Numerical approximation of anisotropic geometric evolution equations in the plane*, [IMA J. Numer. Anal.](#), **28** (2008), 292–330.
- ———, *A variational formulation of anisotropic geometric evolution equations in higher dimensions*, [Numer. Math.](#), **109** (2008), 1–44.
- ———, *Parametric approximation of surface clusters driven by isotropic and anisotropic surface energies*, [Interfaces Free Bound.](#), **12** (2010), 187–234.
- ———, *On the stable discretization of strongly anisotropic phase field models with applications to crystal growth*, [ZAMM Z. Angew. Math. Mech.](#), **93** (2013), 719–732.
- ———, *Stable phase field approximations of anisotropic solidification*, [IMA J. Numer. Anal.](#), **34** (2014), 1289–1327.